FRPRCS11
Joaquim Barros & José Sena-Cruz (Eds)

Efficiency of CFRP NSM strips and EBR laminates for flexural strengthening of RC beams

A. Balsamo[1], A. Bilotta[2], F. Ceroni[3], E. Nigro[4], M. Pecce[5]
[1]Dep. of Structural Engineering, Univ. of Napoli Federico II, via Claudio 2, 80123 Napoli, albalsam@unina.it
[2]Dep. of Structural Engineering, Univ. of Napoli Federico II, via Claudio 21, 80123 Napoli, antonio.bilotta@unina.it
[3]Engineering Dep. Univ. of Sannio, Piazza Roma 21, 82100 - Benevento, ceroni@unisannio.it
[4]Dep. of Structural Engineering, Univ. of Napoli Federico II, via Claudio 21, 80123 Napoli, emidio.nigro@unina.it
[5]Engineering Dep. Univ. of Sannio, Piazza Roma 21, 82100 Benevento, pecce@unisannio.it

Keywords: CFRP; NSM; EBR; Flexural strengthening; Beams; Debonding.

SUMMARY
The efficiency of Fiber Reinforced Polymer (FRP) materials for strengthening existing Reinforced Concrete (RC) structures according to the Near Surface Mounted (NSM) technique can be greater than the External Bonded Reinforcement (EBR) technique since the tensile strength of the FRP materials is in general better exploited.
Firstly, this paper deals with analyzing the effect of the loading pattern on RC beams strengthened with both types of strengthening technique; in particular, two loading patterns have been used for the experimental tests on simple supported beams: 1) a four points bending scheme, and 2) a scheme with distributed loads, in order to check the sensitivity of failure modes and ultimate loads to different distributions of bending moment and shear along the beam. Then, a comparison between the results of flexural tests on RC beams strengthened with both NSM and EBR techniques is dealt with.

1. INTRODUCTION

Several experimental works showed that the tensile strength of the Fiber Reinforced Plastic (FRP) materials can be strongly exploited by the Near Surface Mounted (NSM) technique [1]. In particular bond tests on concrete specimens strengthened either with Externally Bonded Reinforcement (EBR) or with NSM technique showed that the same loads can be achieved for both typologies, even if the NSM-FRP reinforcements are characterized by lower area and stiffness. However, the efficiency of both techniques depends on the bond behaviour, which in the case of the NSM-FRP one is influenced by several parameters as groove dimensions, concrete surface roughness, mechanical properties of FRP materials, type of adhesive [2].
Whatever the strengthening technique, the failure of the strengthened member is often due to debonding of the FRP reinforcement that can take place in different zones of the member [3]. For design/check of flexural strengthening of Reinforced Concrete (RC) beams, both debonding at the end of the external reinforcement (End Debonding, ED) and at the location of bending/shear cracks should be considered. In this last case, the predictive models of the debonding phenomenon depend on the type of crack: a) Intermediate Crack Debonding (ICD), when debonding occurs near flexural cracks in the zones where the bending moment in the beam is maximum, or b) Critical Diagonal Crack Debonding (CDCD) when debonding occurs at shear cracks, usually where the shear is maximum. Since in simply supported beams the shear is maximum close to the ends of the FRP reinforcement, the CDCD can interact with the ED.
Theoretical models for ED are based on results of bond tests, because in the area of anchoring the distributions of bond stresses are similar to those observed in bond tests [1]. Theoretical models for ICD or CDCD are in general based on results of flexural tests [5]. The activation of the debonding mechanisms depends on the geometry of reinforcement (in particular the distance between the support

and the end of the FRP), the loading pattern (distributed or concentrated) and the shear-bending interaction, which can influence the inclination of the cracks and the mechanisms of debonding [6].
Shear bending interaction and loading pattern are clearly correlated. Most of the bending tests available in the literature have been carried out according to the scheme of simply supported beam loaded in 1 or 2 points (3 or 4 points bending test) that are usually easier to be performed in laboratories compared with the application of a distributed load, nevertheless the latter is more likely to actual load conditions. Under concentrated loads both moment and shear are maximum near the mid-span of the beam, while at the anchorage of the FRP reinforcement the moment is minimum and the shear remains constant. Under distributed loads, the shear-moment interaction is lower because at the mid-span the bending moment is maximum and the shear is zero, while at the end of the reinforcement the moment is minimum and the shear is close to its maximum value. This would imply that under distributed loads the ICD should be less relevant than ED, due to the low shear-moment interaction near to the mid-span.
Moreover, it should be noted that in many experimental tests on beams with concentrated loads the debonding was induced by the formation of diagonal cracks that try to join the ends of the FRP reinforcement with the application point of the loads. This type of cracks, often indicated as Critical Diagonal Crack, can also be induced by strong shear stresses in the anchorage area for elements weakly reinforced against shear. Some models consider in fact, for the check against the CDC debonding, the calculation of a shear resistance that has to be compared with the applied shear force [7].
As stated above, few tests were performed on RC beams reinforced with EBR-FRP by applying distributed loads. However, some experimental results [8] and some numerical analyses [9] indicate that the maximum strain in the FRP at beginning of ICD in case of distributed loads is higher than the maximum strain achieved under concentrated loads. This issue was not yet investigated for RC beams reinforced with NSM-FRP. Therefore, in the following sections the effect of the load shape (4 points bending test and distributed loading pattern in a simple supported beam) on the failure of RC beams reinforced with FRP according to EBR technique is investigated. Then, a comparison between the efficiency of the EBR and NSM techniques is briefly showed for the case of distributed loads.

2. EXPERIMENTAL PROGRAM

A total of 8 RC beams were tested as simple supported members over a clear span of 2.1 m. The load was applied according to two different schemes:
a) four-points bending scheme (Figure 1a) with 2 forces at distance of about 25 cm across the mid-span;
b) a distributed loading pattern (Figure 1b) with 8 loading points spaced of 25 cm along the beam axis.
All beams had a rectangular cross section of height 160 mm and width 120 mm, internal steel reinforcement (2 ϕ 10, namely A_s = 1.57 mm^2), steel stirrups (diameter 6 mm) spaced of 200 mm (Figure 2a). The concrete cover is 45 mm for the bottom steel reinforcement and 31 mm for the top one measured in both cases from the centroid of the bars. The quite large spacing of stirrups was chosen in order to reduce their influence on the crack pattern.
The average cubic compressive strength of concrete is 21 MPa, as resulted from four tests on cubic specimens (side 150 mm). Three tensile tests on the steel bars gave an average yielding strength of 540 MPa and an ultimate tensile strength of 590 MPa. The same type of carbon FRP laminate (thickness 1.4 mm, Young's modulus 171 GPa, tensile strength 2052 MPa and maximum strain of 0.012, as obtained by tensile tests on three coupons) was used as strengthening both for the EBR and NSM technique.
For the EBR technique a laminate with a width of 40 mm was glued on the bottom part of the beam (Figure 2b), after the surface has been cleaned with compressed air and a layer of primer was applied. For the NSM technique, strips with width of 10 mm were inserted in grooves with dimensions 5 mm x 15 mm (Figure 2c-d). The grooves were realized with a circular saw. As done for the EBR system, the concrete surfaces were cleaned with compressed air. The same primer and adhesive were used for each application. For all the strengthened beams (4 with EBR and 2 with NSM) the FRP reinforcement was applied at a distance of 100 mm from both supports (see Figure 2a). Table 1 shows the experimental program. Specimens are identified throughout this paper using the R_L_NxTxW_n label, where:

- R indicates the type of reinforcement
- L indicates the type of load
- N is the number of strips
- T is the thickness of the strips
- W is the width of the strips

- n is test cardinal number, to distinguish different tests on similar specimens.

Two beams were tested without any strengthening system to be used as control: one according to the four points bending scheme and one according to a distributed loading pattern. Two EBR beams were loaded up to failure under the four point configuration. Other four beams (two with EBR and two with NSM) were tested with the distributed loading pattern. The load was applied through a universal testing machine under displacement control (0.05 mm/s). The deflection at mid-span was measured by a vertical linear variable displacement transducer. Several strain gauges were glued on the bottom of the EBR reinforcement, while for the NSM systems the strain gauges were glued on a side of the strips before they were inserted and glued in the grooves; the position and label of the strain gauges are reported in Figure 3.

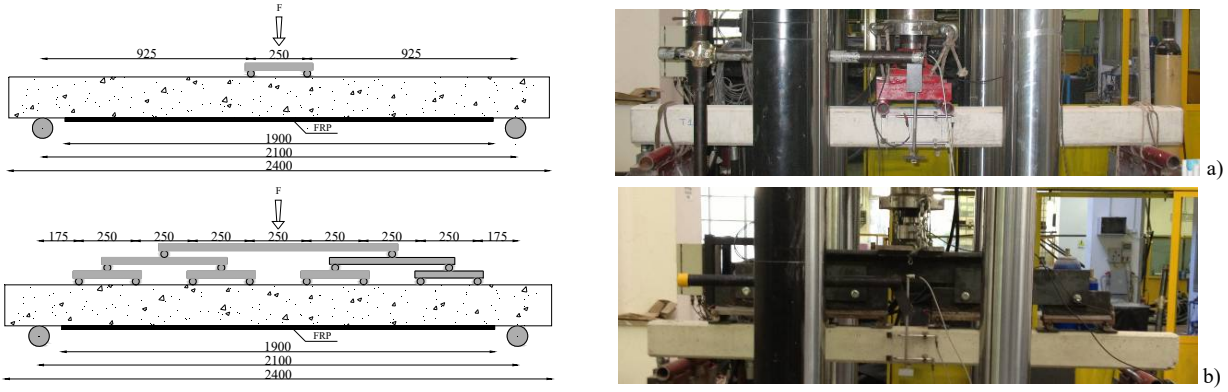

Figure 1: Test set-up: a) four points scheme; b) distributed loading pattern.

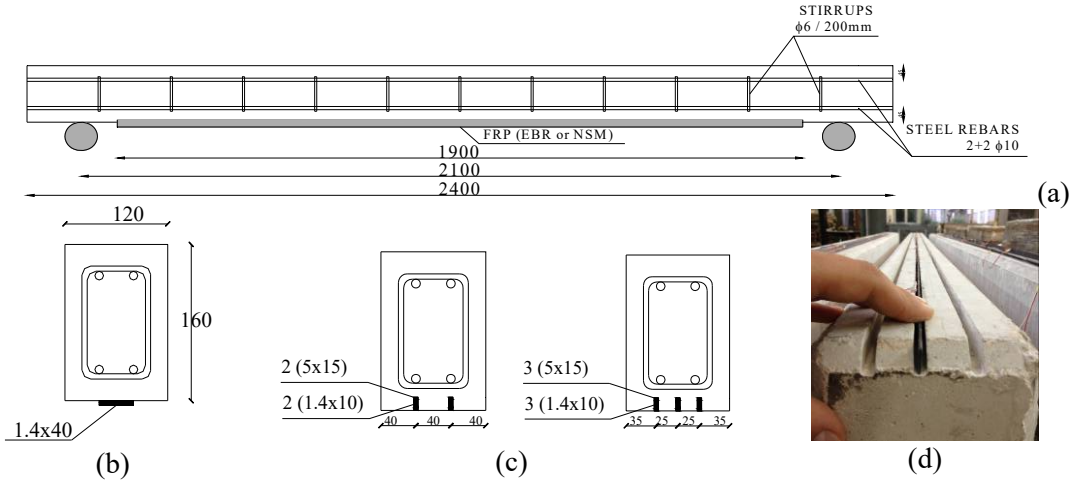

Figure 2: Geometry of the beams and reinforcement scheme: a) longitudinal section; b) transversal section of beams with EBR; c) transversal section of beams with NSM, d) NSM strips in the grooves.

Table 1: The experimental program

Specimen ID	**FRP type**	**FRP Area** [mm^2]	**Loading pattern**	**SG lay-out**
Ref_c_no_1	No	-	concentrated	-
Ref_d_no_1	No	-	distributed	-
EBR_c_1.4x40_1	EBR	56	concentrated	a
EBR_c_1.4x40_2	EBR	56	concentrated	a
EBR_d_1.4x40_1	EBR	56	distributed	a
EBR_d_1.4x40_2	EBR	56	distributed	a
NSM_d_2x1.4x10_1	NSM	28	distributed	b
NSM_d_3x1.4x10_1	NSM	42	distributed	c

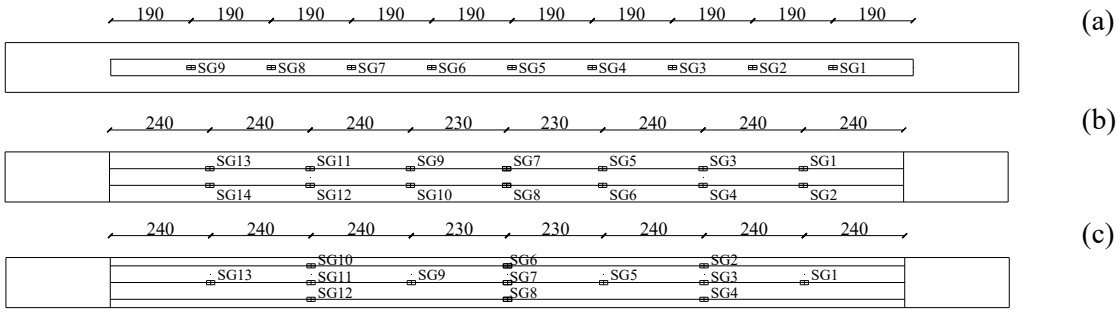

Figure 3: Location of strain gauges on FRP: a) beams with EBR; b) beams with 2 strips; c) beams with 3 strips.

3. DISCUSSION OF RESULTS

3.1 Experimental failure modes and loads

In Table 2 the failure mode, the maximum experimental load, $F_{max,exp}$, recorded for each specimen and the mean value of equal beams, $F_{max,exp,m}$, are reported. Moreover, the bending moment at midspan of the simply supported beam, $M_{max,exp}$, corresponding to $F_{max,exp}$ is also calculated. The different failure modes observed during the tests, are listed and identified in Table 2 and showed for each specimen in Figure 4. Both the un-strengthened beams failed for compression of concrete (CC) after steel yielding (SY) (Figure 4a and b).

In general, the experimental maximum loads in case of distributed loading scheme are larger than those under concentrated loads due to the different load patterns for which the internal forces along the beam are different; indeed, based on the locations of the concentrated forces (see Figures 1a-b), the theoretical ratio of the maximum load in the two schemes to have the same moment at the mid-span should be 1.7. Actually, for the reference beams this ratio is 2.3 ($F_{max,exp}$ is 46.1 kN and 20.1 kN for distributed and concentrated loads, respectively). Note that the moment at mid-span due to the own weight of the beam (equal to about 0.3 kN m) can be considered negligible. Also for the beams strengthened with the EBR plate, the ratio of the maximum loads in the case of distributed and concentrated loads is higher than 1.7, but it is lower than the value obtained for the reference beams (2 vs. 2.3).

Such higher ratios could be due not only to the uncertainties in the geometrical and mechanical characteristics of the beams that have small sizes and, thus, are very sensible to little variations of geometrical and mechanical details (i.e. position of bars, values of yielding stress, hardening of steel), but also to the uncertainties about the effective distribution of the 8 forces in the distributed loading system. Any imperfection in the behaviour of the hinges (Figure 1b) can, indeed, lead to a non uniform distribution of the forces.

In Table 2 the increase of the experimental maximum load, $\Delta F_{max,exp,m}$, in equal strengthened beams respect to the reference one is also listed. The mean load increase is equal or greater than 50% for all types of strengthening, with the higher values achieved in the case of concentrated loading scheme. In particular, it is worth to note that the strength increase, $\Delta F_{max,exp,m}$, attained by the beams with EBR plates under distributed loads is lower (52%) than the one attained under concentrated loads (+78%), i.e. this indicates that the efficiency of the strengthening system depends on the loading pattern. Indeed, nevertheless the maximum strain in the EBR plate at failure is expected to be higher in case of ICD, the effective failure mode for the strengthened beams under distributed loads is an End Debonding with shear-moment interaction.

Looking at the maximum loads achieved by the strengthened beams with NSM strips under distributed loads, the greater efficiency of this strengthening technique is confirmed compared with the EBR [1]; indeed, the failure loads of beams strengthened with the EBR plate and the NSM strips are very similar, even if a lower amount of the same FRP material is used in the case of strips (2 strip = 28mm^2 or 3 strip = 42mm^2 vs. 1 plate = 56mm^2).

Both beams strengthened with the EBR plate and loaded under concentrated forces reached about the same maximum load, even if with slightly different failure modes. Indeed, the first beam failed for contemporary debonding of the FRP plate in the central area (ICD) and at the right end (ED) (Figure 4c), while for the second one only the end debonding of the FRP plate occurred (Figure 4d). Figure 4d shows evidently two cracks at the failed end of the beam: one propagates versus the loading point (Critical

Diagonal Crack) and the other is parallel to the steel reinforcement in tension (that means a Concrete Cover Separation failure). Both cracks did not start exactly from the end of the plate and confirm the interaction between different failure phenomena close to the end of the FRP plate.

Table 2: Experimental failure loads and failure loads.

Specimen ID	Failure Type	$F_{max,exp}$ [kN]	$F_{max,exp,m}$ [kN]	$M_{max,exp}$ [kNm]	$\Delta F_{max,exp,m}$ [%]	Failure modes ID
Ref_c_no_1	CC+SY	20.1	-	9.3	-	CC = Concrete Crushing SY = Steel Yielding SH = Shear failure ED = End Debonding ID = Intermediate Debonding CDCD = Critical Diagonal Crack Debonding CCS = Concrete Cover Separation
Ref_d_no_1	CC+SY	46.1	-	12.7	-	
EBR_c_1.4x40_1	ED-ID	36.5	35.8	16.7	+78	
EBR_c_1.4x40_2	CDCD-CCS	35.2		16.3		
EBR_d_1.4x40_1	ED-CCS	75.1	70.0	19.7	+52	
EBR_d_1.4x40_2	ED	64.8		17.0		
NSM_d_2x1.4x10_1	SH	71.3	-	18.7	+55	
NSM_d_3x1.4x10_1	SH	67.6	-	17.7	+47	

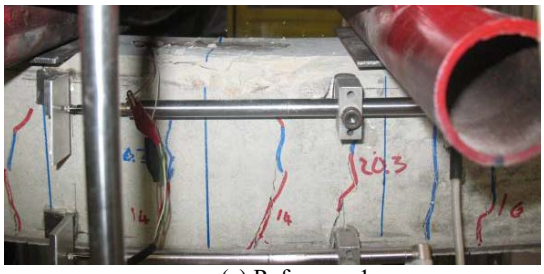

(a) Ref_c_no_1

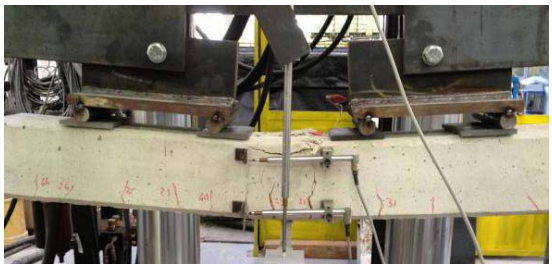

(b) Ref_d_no_1

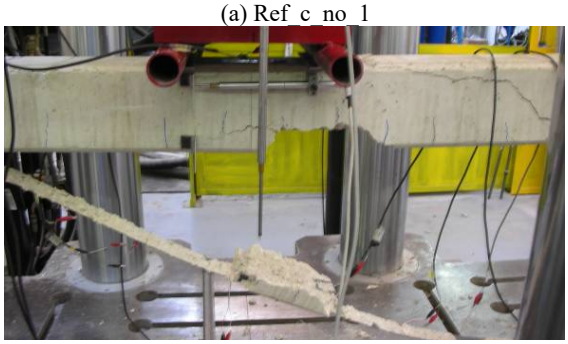

(c) EBR_c_1.4x40_1

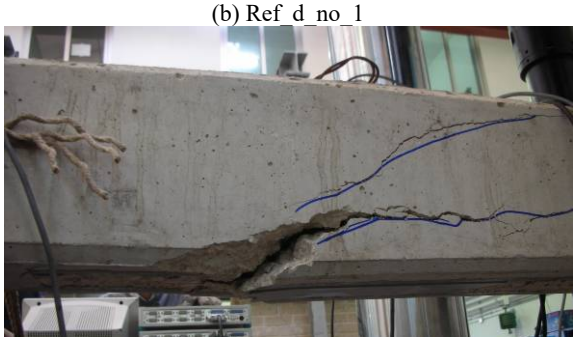

(d) EBR_c_1.4x40_2

(e) EBR_d_1.4x40_1

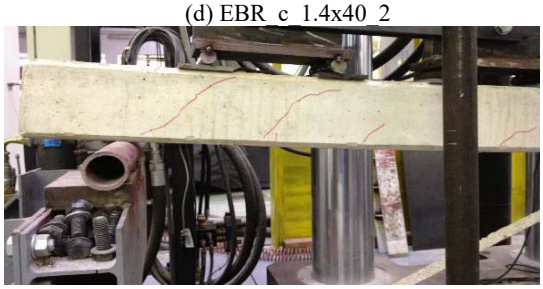

(f) EBR_d_1.4x40_2

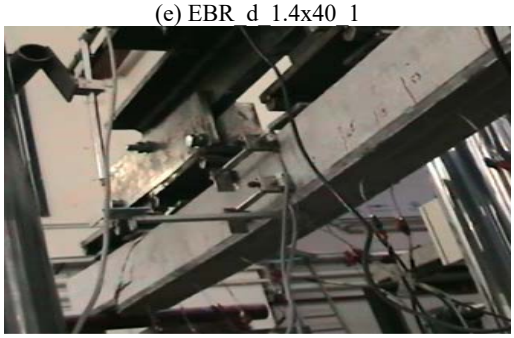

(g) NSM_d_2x1.4x10_1

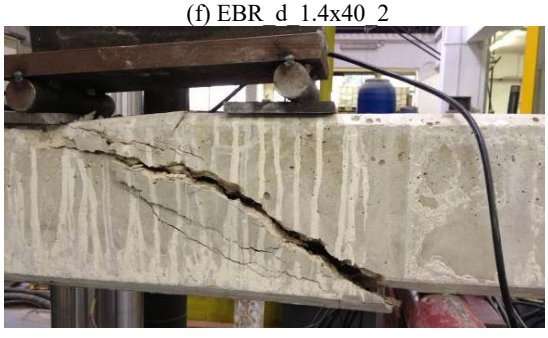

(h) NSM_d_3x1.4x10_1

Figure 4: Failure modes in un-strengthened and strengthened beams.

In the case of distributed loading pattern, the shear attained at the end of the beam is higher than the one attained in the beams tested under concentrated loads for having the same bending moment at the mid-span, while the shear is zero at mid-span where the moment is maximum. Thus, ICD was not achieved, but only ED. Indeed, for the first beam the ED with removal of the concrete cover (CCS) occurred (Figure 4e), while for the second one the failure was simply due to end debonding (Figure 4f). Note also that the CDC failure mode did not occur for these beams probably because of the lower influence of the shear cracks at the ends in the case of distributed loading pattern (shear is decreasing from the end to the mid-span). Moreover, the minor distance of the end of the FRP plate from the application point of the forces (see Figure 1b) avoided the formation of the Critical Diagonal crack (Figure 4e) or made the diagonal crack less critical for the overall behaviour of the beam (Figure 4f).
A completely different behaviour was observed for the beams strengthened with NSM strips: the failure was due to shear (SH) for both beams. This failure mode could be expected because, as already discussed, under the distributed loads the shear at the ends of the beam is greater and therefore the critical failure mode can move from bending to shear, if debonding phenomena do not occur.
The debonding did not occur even at the end of the NSM strips. This confirms that RC beams strengthened with NSM systems are less sensitive to debonding phenomena compared with beams strengthened with EBR plates. Moreover, the slight decreasing of strength when the NSM strips increase (3 instead of 2) can be addressed to experimental scattering, since the shear strength of the beam is not enhanced by the NSM reinforcement, but depends on the mechanical properties of steel and concrete.
Nevertheless the shear failure attained in these beams, caused both by the relevant load increase induced by the loading pattern and by the lower sensitivity of NSM systems to debonding phenomena, the results can be considered satisfactory. Indeed, the aim of the experimental program was comparing the flexural performances of the two strengthening techniques and assessing the effect of the loading scheme.

3.2 Experimental load-deflection behaviour

In Figure 5a the load-deflection curves are plotted for the unstrengthened and the EBR beams in the case of concentrated and distributed loads. In Figure 5b the load-deflection curves are plotted for the unstrengthened and the NSM strengthened beams for distributed loads. The comparison clearly shows that an increase of stiffness is obtained with the FRP plate (1.4mm x 40mm) beyond the strength increase compared with the reference beam. On the other hand, a negligible increase of stiffness is obtained when 2 NSM strips (2 x 1.4mm x 10mm) are used, while the same strength of the beams strengthened with the FRP plate is achieved. The stiffness increases slightly when 3 strips (3 x 1.4mm x 10mm) are applied. The lower efficiency of the NSM systems in terms of stiffness is probably due to the application in the grooves that could lead to have higher slips along the FRP-concrete interface as was evidenced also in [3].

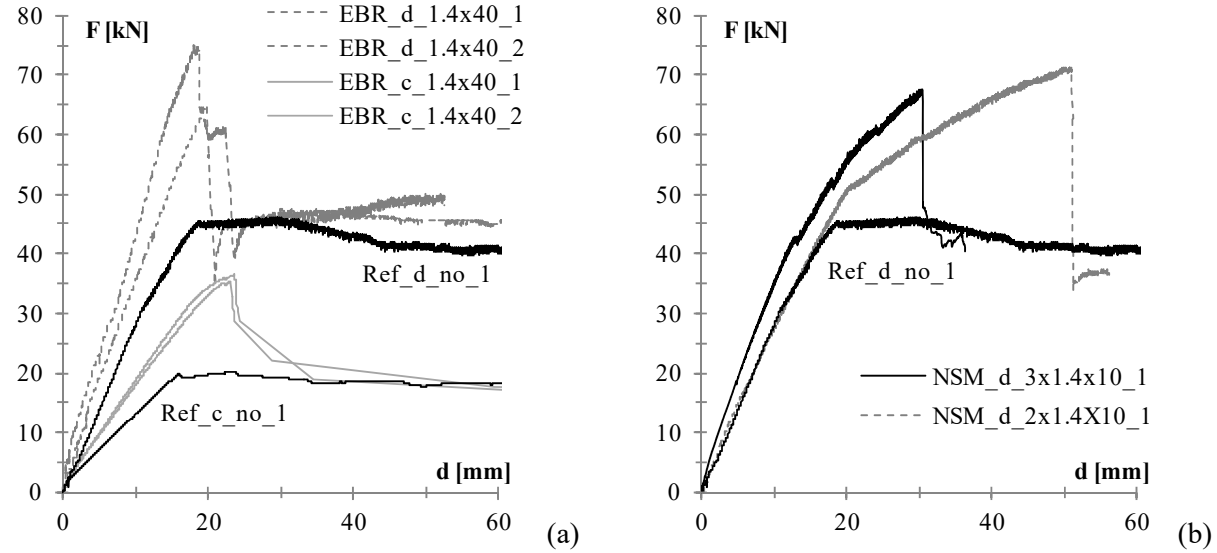

Figure 5: Load-deflection curves: a) reference and EBR strengthened beams under concentrated and distributed loads; b) reference and NSM strengthened beams under distributed loads.

3.3 Theoretical strength predictions

For the un-strengthened beam the theoretical cracking moment is about 0.7 kN m, which is in agreement with the formation of the first cracks experimentally observed during the tests.
For the un-strengthened beam, the force, $F_{max,th}$, necessary to attain the ultimate bending moment $M_{u,th}$ at mid-span is calculated for the two load schemes and is reported in Table 3. The ultimate bending moment, $M_{u,th}$, is calculated under the hypothesis of concrete crushing ($\varepsilon_{c,u}$ = 0.0035, f_{cm} = 17.4 MPa) and considering both the yielding (f_y = 540 MPa) and the ultimate tensile strength (f_u = 590 MPa) of the steel reinforcement. The theoretical maximum loads are in good agreement with the experimental ones under concentrated forces (see Table 2). On the contrary, in the case of distributed loads, the experimental maximum moment is sensibly higher (about 13 kN m) than the theoretical one (about 8 kN m); as previously discussed, this higher experimental strength could be caused by some imperfections in the behaviour of the hinges of the loading system that could have led to an uniform distribution of the forces applied in the 8 loading points.
Moreover, the shear strength $V_{u,th}$ of the unstrengthened beam is also calculated by considering a truss resistant mechanism with variable angle θ for the concrete struts. For the angle θ= 22° the contemporaneous failure of steel stirrups and concrete struts theoretically occurs; the shear strength corresponding to this condition is 36.2 kN and, thus, the related maximum force, $F_{max,th}$, is 72.4 kN.

Table 3: Theoretical maximum moments and forces for the un-strengthened beams

Section: Mid-span, x = 1050 mm	$M_{cr,th}$ [kN m]	$M_{y,th}$ [kN m]	$M_{u,th}$ [kN m]
	0.69	7.96	8.53
4 points: $F_{max,th,4}$ [kN]	1.5	17.3	18.6
Distributed: $F_{max,th,d}$ [kN]	2.5	28.9	31.0

For the beams strengthened with EBR plates, the theoretical loads associated both to the End and to the Intermediate Crack Debonding (ED and ICD) are considered according to the approach suggested in the new draft of CNR DT 200/2012 [10]. In particular, the mean values of the maximum strain in the FRP plates are calculated according to the following expressions:

End debonding (ED)

$$\varepsilon_{\max,FRP} = \sqrt{\frac{2 \cdot k_b \cdot 0.063 \cdot \sqrt{f_{cm} \cdot f_{ctm}}}{E_f \cdot t_f}} \qquad k_b = \max\left(1; \sqrt{\frac{2 - b_f/b}{1 + b_f/b}}\right)$$
$$L_{eff} = \frac{\pi \cdot s_u}{2} \cdot \sqrt{\frac{E_f \cdot t_f}{2 \cdot k_b \cdot 0.063 \cdot \sqrt{f_{cm} \cdot f_{ctm}}}} \qquad s_u = 0.25\,mm \tag{1}$$

Intermediate debonding (ID)

$$\varepsilon_{\max,FRP} = k_q \cdot \sqrt{\frac{2 \cdot k_b \cdot 0.32 \cdot \sqrt{f_{cm} \cdot f_{ctm}}}{E_f \cdot t_f}} \qquad k_q = \begin{cases} 1.00 & \text{for concentrated loads} \\ 1.25 & \text{for distributed loads} \end{cases} \tag{2}$$

b is the beam width, E_f, t_f, b_f are Young's modulus, thickness and width of the FRP reinforcement

For the ICD the maximum strain in the FRP reinforcement given by Eq. (2) is used for calculating the ultimate moment $M_{u,th}$ corresponding to the debonding of the strengthening system. The value of $F_{max,th}$ corresponding to $M_{u,th}$ is reported in Table 4 for both loading schemes. Note that the amplification of the maximum strain by the factor k_q = 1.25 under distributed loads leads to have a greater theoretical ratio $F_{\max,th,d}/F_{\max,th,4}$ compared to the case of the un-strengthened beams (1.83 vs. 1.67).
For the ED, the maximum strain in the FRP reinforcement given by Eq. (1) refers to the 'anchorage' section that is distant L_{eff} from the plate end; for the examined FRP plate L_{eff} = 230 mm and, thus, the section is distant x = 100 mm + 230 mm = 330 mm from the support. $M_{u,th}$ was calculated in this case through the Navier's formula with the assumption of linear elastic behaviour of materials due to the lower stress condition at the anchorage section. The value of $F_{max,th}$ corresponding to $M_{u,th}$ is reported in Table 4 for both loading schemes. Note that for the ED the ratio $F_{\max,th,d}/F_{\max,th,4}$ is only 1.13, due to the very similar values of bending moment at the anchorage section, for both loading patterns.
It has to be noticed that, the theoretical strength increase under distributed loads for the beams with EBR plates respect to the yielding load of the reference beams is 32% (38.1 kN vs 28.9 kN) in case of ED or

72% (49.8 kN vs 28.9 kN) in case of ICD; on the contrary, for the beams under concentrated force the theoretical strength increase is 95% (33.7 kN vs 17.3 kN) for ED and 57% (27.2 kN vs 17.3 kN) for ICD. These results show that the efficiency of the strengthening system depends on the loading pattern and on the failure modes, as already observed in the discussion of the experimental results; i.e. the theoretical ED load is lower than the ICD one in the case of distributed loads, while it is higher in the case of concentrated loads. This would mean a lower efficiency of the FRP plate under distributed loads for the ED failure; actually, the experimental results have shown a strength increase for the beams tested under distributed loads higher than the theoretically predicted one (52% vs. 31%), probably due, as already observed, to a not uniform distribution of the 8 forces that the loading system is made of. Indeed, the experimental debonding loads for the beams tested under concentrated loads are lightly larger than the theoretical ED and ICD loads. On the other hand, the debonding loads for the beams tested under distributed loads are very higher than the theoretical ED and ICD ones, although the maximum strain in the plate for ICD has been also amplified of 1.25 for the distributed loading scheme.

Table 4: Theoretical provisions for EBR strengthened beams

Failure mode	Section	$\varepsilon_{max,FRP}$ [-]	$M_{u,th}$ [$kN\,m$]	4 points $F_{max,th,4}$ [kN]	Distributed $F_{max,th,d}$ [kN]	$F_{max,th,d}/F_{max,th,4}$
ED	Anchorage section x = 330 mm	0.0017	5.6	33.7	38.1	1.13
ICD	Mid-span: x = 1050 mm	0.0038*	12.5	27.2	45.5*	1.67
		0.0048**	13.7		49.8**	1.83
CC	Mid-span: x = 1050 mm	0.0065	15.7	34.1	57.1	1.67

* not increased for distributed load, ** increased for distributed load

For CC failure mode, if the maximum strain in the concrete is limited to the conventional value 0.0035 and the steel is assumed yielded, the strain in FRP is lower than the maximum tensile strain (0.012). The values reported in Table 4 are calculated under this hypothesis. However, this kind of failure did not occurred in any strengthened beams and the experimental measures of the maximum strain in the concrete are higher than 0.0035.
For the beams strengthened with NSM strips two failure modes were considered: failure of the strips in tension (TF) and End Debonding (ED). The maximum tensile strain for TF is the same of the EBR, being the material the same (0.012), while for ED the following expression [11] is adopted:

$$\varepsilon_{\max,th} = a \cdot \frac{\left(p_{f,g}\right)^c}{\left(E_f \cdot A_f\right)^b} \qquad \text{with } a = 272,\ b = 0.85,\ c = 0.71 \tag{3}$$

$p_{f,g}$ and A_f are the perimeter of the groove and the transversal area of the NSM reinforcement

The Eq. (3), for the mechanical and geometrical properties of the tested strips, gives a maximum strain of 0.013 at the end, whereas the maximum tensile strain is 0.012. This means that the strengthened beam, theoretically, should fail at the midspan section for tension failure of the fibres. Moreover, assuming the internal steel reinforcement yielded and limiting the maximum strain in the compressed concrete to 0.0035, the tensile failure in the strips cannot be achieved, as in the case of EBR plate; the maximum strains that 2 or 3 strips can achieve under these hypothesis are reported in Table 5 together with the corresponding value of $M_{u,th}$ and $F_{max,th,}$.

Table 5: Theoretical provisions for NSM strengthened beams

Failure mode	NSM reinforcement	Section	$\varepsilon_{max,FRP}$ [-]	$M_{u,th}$ [kNm]	$F_{max,th,d}$ [kN]
TF	2 x 10 x 1.4	Mid-span:	0.008	13.0	47.5
	3 x 10 x 1.4	x = 1050 mm	0.007	14.5	52.8

The maximum experimental loads achieved by both beams strengthened with NSM strips and tested under distributed loads are greater (meanly +10%) than the theoretical ones related to bending failure, but the actual failure mode is due to shear. The flexural strength of the beam is underestimated due also to the hypothesis of limiting the maximum strain in the concrete to 0.0035. On the contrary, the

theoretical shear strength previously calculated for θ=22° (72.4 kN) is comparable with the experimental maximum loads (about 70 kN).

3.4 Experimental vs. theoretical strains

In Figure 6 the strain distributions are reported for the two beams tested under the concentrated loading scheme at five levels: 0.2, 0.4, 0.6, 0.8 F_{max}, and F_{max}; at the same loads the theoretical strains calculated according to the Navier's formula are also graphed. The comparisons show that up to about 28 kN (i.e. 0.8 F_{max}) the experimental and theoretical strains agree quite well, even if the experimental ones are lightly lower than the theoretical ones, probably due to slips along the concrete-FRP plate interface. As the maximum load approaches, the experimental strains overcome the theoretical ones; this phenomenon is probably caused by the two concentrated forces that could locally modify the strength behaviour as the load increases (e.g. introducing a strut and tie mechanism instead of a 'beam' behaviour) and lead to an increase of strains in the FRP plate.
The strains measured close to failure (about 36 kN) are also reported in Figure 6 together with the theoretical values corresponding to ED and ICD [10]; the comparisons show that the experimental values are greater than the theoretical ones both at the end of the FRP reinforcement (ED) and at sections close to the mid-span (ICD). This agrees with the experimental evidence: one beam failed for ED, while the other one had a contemporaneous ED and ICD failure. Moreover, the experimental strains at mid-span are equal to the theoretical ICD ones at about the same load (27-28 kN); since the failure in both beams occurred at higher loads (36 kN), the code provisions [10] for ICD are safe.

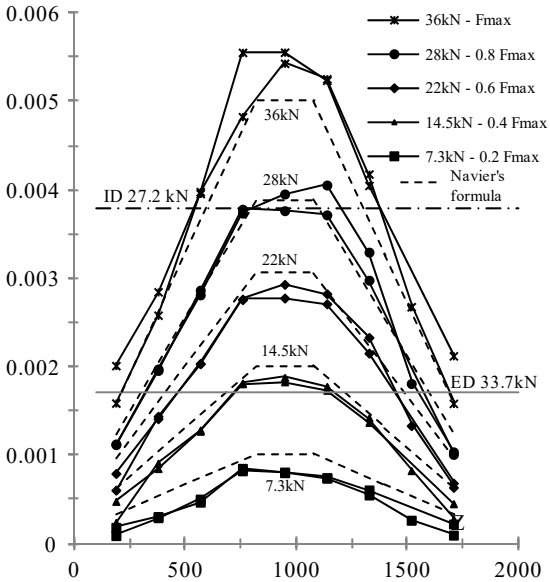

Figure 6: Strain distributions for EBR beams under concentrated forces.

4. CONCLUSIONS AND FUTURE WORK

Even if some experimental results and numerical analyses performed in the past showed that the bond strength in RC beams reinforced with EBR-FRP could be influenced by the effect of the loading pattern, most of bending tests have been realized according to a 3 or 4 points loading scheme and very few tests have been performed under distributed loads. This issue was not yet investigated for RC beams reinforced with NSM-FRP.
Therefore, the effect of the loading pattern (4 points or distributed loading pattern in a simple supported scheme) on the failure loads and modes of 8 RC beams externally reinforced with a carbon FRP plate or with NSM carbon strips, made of the same material, was investigated in this paper.
Different debonding failures for the beams strengthened with the carbon FRP plate are discussed (Intermediate Crack Debonding, End Debonding, Critical Diagonal Crack Debonding) and the experimental maximum loads are compared with the theoretical ones, obtained through existing failure models, both for the case of 4 points and distributed loads. The theoretical formulations appear in general reliable for the beams tested under the 4 points scheme, both for ED and ICD, as expected

because these formulations were calibrated on similar bending tests, while they seem to be significantly safe for the beams tested under distributed loading pattern. Actually, this could be caused also by a not uniform distribution of the 8 forces that the distributed loading system is made of.
Moreover, it is worth to note that both the theoretical predictions and the experimental results evidenced a lower efficiency of the EBR plate, evaluated as flexural strength increase respect to the reference beam, under distributed loads respect to the 4-points scheme. Under distributed loads, indeed, a relevant flexural strength increase was obtained for the reference beam compared to the 4-points scheme, while the failure mode in the strengthened beams shifted from ICD to ED.
The comparisons of the strains measured along the FRP plate for the beams under 4-points scheme with the ones given by the Navier's formula have evidenced that the experimental and the theoretical values are comparable, even if the experimental ones become higher as the load increases, probably due to additional strength mechanisms (e.g. strut and tie). Further investigations need for assess the behaviour of the beams under distributed loads, since, as already discussed, there are some uncertainness about the effective values of the forces applied by means of the distributed loading system.
A greater efficiency in terms of flexural strength increasing is evidenced when NSM strips are used compared to the EBR plate: nevertheless the lower transversal area, the maximum loads of both beams strengthened with 2 or 3 NSM strips is, indeed, comparable with the ones achieved by the EBR beams under the distributed loading pattern and the failure is due to shear instead of debonding. These first results evidence that the debonding phenomena in beams strengthened with NSM strips are less significant compared with EBR beams. Moreover, the experimental results seem to indicate also that the NSM strips are less effective in reducing the beam stiffness compared with the EBR plates.
Therefore, further theoretical and experimental investigations should be devoted in the future to better show the effect of the loading pattern on debonding phenomena in beams strengthened with both EBR and NSM systems.

ACKNOWLEDGMENTS

The author would like to thank Mapei SpA for providing the FRP materials and resins used in the experimental program.
The experimental activities have been carried out within the 2010-2013 DPC Reluis project.

REFERENCES

[1] Bilotta A., Ceroni F., Nigro E., Di Ludovico M, Pecce M., Manfredi G. (2011). “Bond efficiency of EBR and NSM FRP systems for strengthening of concrete members”, J. of Composites for Construction, ASCE, 15 (5), 757–772.
[2] Ceroni F., Bilotta A., Nigro E, Pecce M., (2012). “Bond behaviour of FRP NSM systems in concrete elements”, Composites: Part B 43, Elsevier, 99–109.
[3] Ceroni F. (2010). “Experimental performances of RC Beams Strengthened with FRP materials”, Construction and Building Material, Elsevier, 24, 1547–1559.
[4] Teng J.G., Chen J.F., Smith S.T., Lam L., FRP-strengthened RC structures. Chichester, West Sussex, UK: John Wiley and Sons, 2002. p. 245.
[5] Bilotta A., Faella C., Martinelli E., Nigro E., (2013). “Design by testing procedure for intermediate debonding in EBR FRP strengthened RC beams” Engineering Structures, Elsevier, 46, 147–154.
[6] Mazzotti C., Savoia M. (2009). “Experimental Tests on Intermediate Crack Debonding Failure in FRP – Strengthened RC Beams”, Advances in Structural Engineering, 12 (5).
[7] Teng J.G., Yao J. (2007). “Plate end debonding in FRP-plated RC beams—II: Strength model”, Engineering Structures, Elsevier, 29, 2472–2486.
[8] Pan J., Chung T.C.F., Leung C.K.Y. (2009). “FRP Debonding from Concrete Beams under Various Load Uniformities”, Advances in Structural Engineering, 12 (6).
[9] Bilotta A., Faella C., Martinelli E., Nigro E., (2012). “The influence of the load condition on the intermediate debonding failure of EBR-FRP strengthened RC beams”, Proc. of 6th Int. Conf. on FRP Composites in Civil Engineering (CICE 2012), Rome, June 13-15 2012, Italy.
[10] CNR DT 200/R1 (2012). “Guide for the Design and Construction of Externally Bonded FRP Systems for Strengthening Existing Structures”, National Research Council, Advisory Committee on Technical Regulations for Constructions, July, Rome, Italy.
[11] Ceroni F., Pecce M., Bilotta A., Nigro E. (2012). “Bond behavior of FRP NSM systems bonded over concrete elements”, Proc. of 4th Int. Symposium Bond In Concrete, Bond, Anchorage, Detailing, Brescia, 17-20 June 2012, Italy.